J. Phys. C: Solid State Phys., 17 (1984) 5473–5489. Printed in Great Britain

Crystalline and fluid order on a random topography

Subir Sachdev and David R Nelson
Department of Physics, Harvard University, Cambridge, Massachusetts 02138, USA

Received 21 February 1984

Abstract. The statistical mechanics of particles embedded in a surface with quenched fluctuations in its topography is considered. If the fluctuations are not too violent, stable crystalline phases are possible at finite temperatures, with elastic constants renormalised from their flat-space values. Point dislocations and disclinations couple only to the intrinsic gaussian curvature of the surface. Other effects of the surface can be gauged away, just as in Mattis models of spin glasses. At sufficiently low temperatures, crystalline arrays must melt re-entrantly via a dislocation instability. The resulting hexatic phase is also unstable at low temperatures. The random-topography problem is similar in many respects to that of particles in flat space disrupted by a quenched random array of impurities.

1. Introduction

There is considerable current interest in frustration, defects and their effects on crystalline and fluid order at low temperatures (Yonezawa and Ninomiya 1983). These studies are motivated by the hope of ultimately understanding the structure and statistical mechanics of amorphous materials. It has been argued recently that metallic glasses and supercooled liquids in three dimensions are strongly defected states of a medium with local icosahedral bond orientational order (Steinhardt *et al* 1983, Nelson 1983a, b, Sethna 1983, Nelson and Widom 1984). The defect density in the ground state goes to zero when the medium is embedded in a three-dimensional space with uniform positive curvature (Coxeter 1969, 1973). Flat three-dimensional space is 'frustrated' because it does not allow the formation of a irregular icosahedral solid; defects such as disclinations are inevitable (Kleman and Sadoc 1979). Flat two-dimensional space, on the other hand, readily allows formation of regular hexagonal solids. Because analytic theories of melting in two dimensions are available (Halperin and Nelson 1978, Nelson and Halperin 1979, Young 1979), it is useful to consider frustrated two-dimensional solids and study the phases that are induced by the frustration. By 'frustration', we mean that particles in the ground state cannot simultaneously sit in the minima presented to them by pairwise interactions with their neighbours. Various mechanisms for introducing frustration in two dimensions have been considered. Motivated by an analogy with frustrated icosahedral order in three-dimensional flat space there have been numerical studies of frustrated hexagonal order on two-dimensional surfaces of constant negative curvature (Rubinstein and Nelson 1983). Experimental and analytical investigations on arrays frustrated by introducing inhomogeneous particle sizes have also been carried out (Nelson *et al* 1982, Nelson 1983b).

0022-3719/84/305473 + 17 $02.25

In this paper we introduce frustration into two-dimensional particle configurations in another way, by embedding them in a randomly corrugated surface. Cooling on such a manifold has been suggested by Gaspard *et al* [1982] as a way of generating amorphous particle configurations. The long-wavelength equilibrium statistical mechanics of a continuum elastic version of this model turns out to be soluble by renormalisation-group methods. The results are insensitive to the kind of fluctuations assumed for the surface. Direct experimental reaslisations may be possible, by quenching a viscous liquid such as molten quartz in equilibrium with a vapour below its glass transition, and then adsorbing large particles (of size 100 Å, say) at the interface. We require the wavelength of quenched fluctuations to be much longer than the interparticle spacing, and the forces confining the particles to the interface to be *normal* to the surface. Although short-wavelength fluctuations in the surface may be present immediately after the quench, we expect that these will be rapidly eliminated by diffusion. The long-wavelength fluctuations we require will persist on laboratory timescales, however, below the glass transition temperature of the quartz.

As pointed out by Gaspard *et al* (1982) the gaussian curvature (Coxeter 1969), $K(\boldsymbol{r})$, of the surface couples to disclinations in the embedded particle configuration. These authors derived a microscopic relation between the distribution of disclinations and the integral of the gaussian curvature in a region S, namely

$$\sum_z (6 - Z) N_Z = \frac{3}{\pi} \int\int_S g^{1/2} \, \mathrm{d}^2 r \, K(\boldsymbol{r})$$

Here N_Z is the number of atoms with coordination z in the region, and $K(\boldsymbol{r})$ is the local gaussian curvature of the surface with metric g. On a surface that is locally flat, most atoms will be six-coordinated and the anomalous five-coordinated and seven-coordinated particles may be viewed as microscopically defined disclinations. A non-zero net gaussian curvature in some region evidently forces in atoms with a coordination number different from six, i.e. disclinations.

A long-wavelength version of this effect emerges from the continuum elastic model considered here. The continuum elastic free energy for a crystal embedded in a slightly curved surface in the harmonic approximation is (Landau and Lifshitz 1970)

$$F = \tfrac{1}{2} \int \frac{\mathrm{d}^2 r}{a^2} (2\mu \tilde{u}_{ij}^2 + \lambda \tilde{u}_{kk}^2)$$

where

$$\tilde{u}_{ij}(\boldsymbol{r}) = u_{ij}(\boldsymbol{r}) + \tfrac{1}{2} A_{ij}(\boldsymbol{r}) \tag{1.2b}$$

and $\boldsymbol{r} = (x, y)$ are coordinates in a reference *flat* surface. The quantity u_{ij} is the strain tensor due to the component of the displacement of the atoms in the reference plane and a is a short-wavelength cut-off (see figure 1). The tensor A_{ij}, which couples to gradients of the displacements in a manner reminiscent of a vector potential, is

$$A_{ij} = (\partial f / \partial x_i)(\partial f / \partial x_j) \tag{1.3}$$

where $f(x, y)$ is the height of the corrugated surface relative to the reference plane. If the discreteness of the underlying lattice can be neglected, the total disclination density $s^{\mathrm{T}}(\boldsymbol{r})$ in the ground state is easily shown to be (see § 2).

$$s^{\mathrm{T}}(\boldsymbol{r}) = \det(\partial^2 f / \partial x_i \partial x_j) = K(\boldsymbol{r}) \tag{1.4}$$

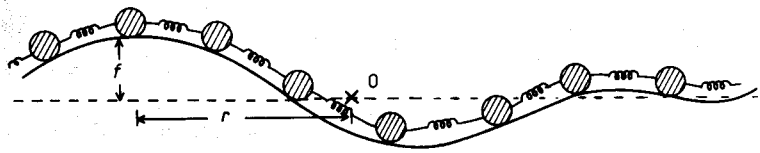

Figure 1. An array of atoms on a random topography. f measures the displacement of the surface from a reference flat surface and r is a coordinate in the reference surface.

which is a continuum version of (1.1). Only the 'intrinsic' curvature enters (1.4). Other effects of the surface can be 'gauged away' be redefining the displacement field, in analogy with Mattis models of spin glasses (Mattis 1976).

We will consider two models for the probability distribution of the shape of the surface. These are described below.

(i) A 'rough surface' (Weeks 1980) which has a distribution

$$\mathcal{P}_{\mathrm{I}}(f(\boldsymbol{r})) \propto \exp\left(-\frac{1}{2T_{\mathrm{f}}}\int |\nabla f|^2 \frac{\mathrm{d}^2 r}{a^2}\right). \tag{1.5}$$

Such a surface is created when there is an energy cost in increasing the area of the surface. Quartz rapidly cooled from the melt should produce a surface with long-wavelength fluctuations governed by this distribution. The 'fictive temperature' T_{f} is a dimensionless ratio of the quenching temperature and the surface tension.

(ii) A 'smooth surface' with a distribution

$$\mathcal{P}_{\mathrm{II}}(f(\boldsymbol{r})) \propto \exp\left(-\frac{1}{2T_{\mathrm{f}}}\int \left(\frac{f}{a}\right)^2 \frac{\mathrm{d}^2 r}{a^2}\right) \tag{1.6}$$

has fluctuations that are more constrained. Here each point of the surface has independent gaussian fluctuations about the reference plane. A surface with fluctuations of this kind might be obtained by rapidly freezing a vapour–crystal or liquid–crystal interface initially in equilibrium below its roughening temperature (Weeks 1980).

Provided the surface fluctuations are not too violent, there is a finite band of temperatures such that a crystalline solid described by (1.2) is stable. In this temperature range, the quenched randomness introduces only a finite renormalisation in the long-wavelength elastic constants. The strains induced by the random topography are screened out by thermally activated bound dislocation pairs. At sufficiently low temperatures this screening is less effective, and we find that the crystal melts re-entrantly via a dislocation-unbinding transition. Some qualitative insight into the physics at low temperatures can be obtained by considering the distributions of gaussian curvature induced by (1.5) and (1.6). In § 3 we show that

$$\mathcal{P}(K(q)) \propto \exp\left(-\frac{\alpha}{2T_{\mathrm{f}}^2}\sum_q \frac{\tilde{K}(q)\tilde{K}(-q)}{q^4}\right) \tag{1.7a}$$

where

$$\tilde{K}(q) = \frac{a}{\Omega^{1/2}}\int \frac{\mathrm{d}^2 r}{a^2} K(\boldsymbol{r}) \exp(\mathrm{i}\boldsymbol{q}\cdot\boldsymbol{r}) \tag{1.7b}$$

and

$$\alpha = \begin{cases} 64/\pi^5 & \text{for smooth surfaces} \\ 64/3\pi & \text{for rough surfaces.} \end{cases} \tag{1.7c}$$

The sum on q extends over the first Brillouin zone. Ω is the area of the surface and we have imposed periodic boundary conditions. The probability functional (1.7) describes a continuous distribution of disclination charges with density $K(r)$. Such a distribution of disclinations occurs, for example, in equilibrium two-dimensional isotropic liquids at long wavelengths well above the melting temperature (Nelson 1982). We shall be interested in how a *frozen* distribution of this kind interacts with discrete point disclination and dislocation charges in a crystal. The dislocation instability mentioned above occurs when a proliferation of unbound dislocations (i.e. disclination dipoles) attempts to compensate the frozen distribution $K(r)$. Instabilities such that the compensation is carried out by unbound disclinations also exist.

In § 2 the continuum elastic model is derived in detail and the effects of the surface on the long-wavelength phonon modes neglecting defects are worked out. Defects are introduced by § 3, where we show how they interact with each other and the gaussian curvature of the surface. The defect part of the free energy turns out to be identical to a recently solved model of solid films on a flat surface with quenched random impurities (Nelson 1983b). The effect of the disorder on phonon excitations in the absence of defects is somewhat different however. Both this system and a crystal embedded in a random topography will exhibit a dislocation-driven re-entrant melting instability into a hexatic fluid at sufficiently low temperatures, provided no other instability intervenes. We go on to examine the renormalisation of the disclination core energy in the resulting hexatic liquid. If dislocations remain in equilibrium, we find that this core energy is driven *negative* suggesting a further instability into an *isotropic* liquid at low temperatures. This conclusion also applies to flat-space films with quenched random impurities.

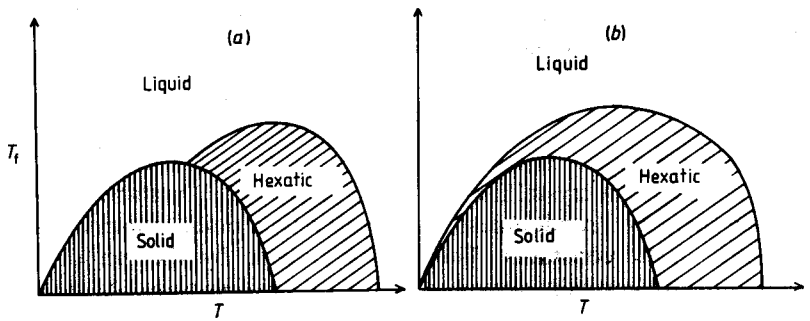

Figure 2. Two possible phase diagrams of the system. T is the temperature and T_f is a quantity measuring the randomness of the surface. Our treatment does not enable us to state whether the low-temperature hexatic phase will be completing pre-empted (figure 2(*a*)) or whether it will exist in a small band between the solid and the liquid (figure 2(*b*)).

Two possible phase diagrams suggested by this analysis are shown in figure 2. The equilibrium low-temperature fluid phases are interesting, because their dynamics presumably becomes increasingly sluggish as they are cooled. One might expect a *gradual* transition to 'glassy' behaviour as $T \rightarrow 0$, with simple Arrhenius divergences in the transport coefficients.

2. The model

2.1. Derivation

Consider an array of identical atoms interacting via a simple pair potential in a flat plane. The ground state will be an unfrustrated hexagonal lattice. We imagine creating a corrugated surface by raising each point (x, y) to a vertical height $f(x, y)$. The atoms are now allowed to relax by movements with surface only. When an atom at $(x, y, f(x, y))$ moves it will change its coordinates to $(x + u_x, y + u_y, f(x + u_x, y + u_y))$. The system is now frustrated because, for a large class of surfaces $f(x, y)$, not all of the near-neighbour bond lengths will be able to relax to equality. The resulting strains tend to produce dislocation and disclination defects. The free energy describing the corrugated state can depend only on changes in bond lengths between atoms (Landau and Lifshitz 1970). Consider two atoms at positions $(x, y, 0)$ and $(x + dx, y + dy, 0)$ before the surface is raised. After the surface has been raised and the atoms are allowed to move on the surface; the new distance between them will be given by

$$ds^2 = g_{kl}\,dx_k\,dx_l \tag{2.1}$$

where

$$g_{kl} \equiv \delta_{kl} + \tilde{g}_{kl} = \left(\delta_{ik} + \frac{\partial u_i}{\partial x_k}\right)\left(\delta_{il} + \frac{\partial u_i}{\partial x_l}\right) + \frac{\partial f}{\partial x_i}\frac{\partial f}{\partial x_j}\left(\delta_{ik} + \frac{\partial u_i}{\partial x_k}\right)\left(\delta_{jl} + \frac{\partial u_i}{\partial x_l}\right). \tag{2.2}$$

The free energy of the bent surface is a functional of the deviation $\tilde{g}_{kl}(x, y)$ of the metric from flatness (see e.g. Kroner 1981). In the ground state the system will try to minimise its energy by reducing $\tilde{g}_{kl}$ to 0 everywhere. In general this can happen only if the system introduces a continuous distribution of defects in the crystal. Since in the presence of defects the displacement field u_i can become multiple-valued we replace $\partial u_i/\partial x_k$ by the distortion tensor w_{ik}:

$$w_{ik} \equiv `\partial u_i/\partial x_k' \tag{2.3}$$

where the quotation marks mean that δ-function contributions due to the cuts in u_i have been subtracted out (Kosevich 1979). The defects give rise to a transverse part of w_{ik}. w_{ik} would be purely longitudinal in the second index k if u_i were single-valued. If we now represent all the second-rank tensors as matrices, (2.2) can be rewritten as a matrix equation:

$$\mathbf{1} + \tilde{\mathbf{g}} = \mathbf{W}^{\mathrm{T}}\mathbf{W} + \mathbf{W}^{\mathrm{T}}\mathbf{A}\mathbf{W} \tag{2.4a}$$

where

$$W_{ij} = \delta_{ij} + w_{ij} \tag{2.4b}$$

and A_{ij} was defined in (1.3). The free energy is minimised when $\tilde{\mathbf{g}} = \mathbf{0}$, i.e.

$$\mathbf{W} = \mathbf{W}^0 = (\mathbf{1} + \mathbf{A})^{-1/2}. \tag{2.5}$$

Upon summing the Taylor series expansion of $(\mathbf{1} + \mathbf{A})^{-1/2}$, we find

$$w^0_{ij} = (\partial f/\partial x_i)(\partial f/\partial x_j)\,F(|\nabla f|^2) \tag{2.6a}$$

where

$$F(\zeta) = (1/\zeta)[(1 + \zeta)^{-1/2} - 1]. \tag{2.6b}$$

The symmetrised strain tensor in this ground state is thus

$$u_{ij}^0 = \tfrac{1}{2}(w_{ij}^0 + w_{ji}^0) = (\partial f/\partial x_i)(\partial f/\partial x_j)\, F(|\nabla f|^2). \tag{2.7}$$

A portion of the strain u_{ij}^0 can be absorbed into simple displacements u_i^0 of the atoms on the surface. Measuring displacements relative to the u_i^0 is like making a 'gauge transformation' on the system. Any two-dimensional second-rank symmetric tensor can be written as the sum of two parts (see e.g. Arnowitt *et al* 1962):

$$u_{ij}^0 = u_{ij}^{\mathrm{T}} + u_{ij}^{\mathrm{L}}. \tag{2.8}$$

The longitudinal part is of the form

$$u_{ij}^{\mathrm{L}} = \partial_i h_j + \partial_j h_i \tag{2.9}$$

for some field $h_i(x, y)$. Clearly this is the pure 'gauge' part of the strain and can be eliminated by a simple displacement $\boldsymbol{u}^0(x, y) = \boldsymbol{h}(x, y)$. Defects in the ground state, which cannot be accommodated by a single-valued set of displacements, are determined by the transverse part of the strain u_{ij}^{T}. In Fourier space, u_{ij}^{T} is of the form

$$u_{ij}^{\mathrm{T}} = (\delta_{ij} - k_i k_j/k^2)\, v(k). \tag{2.10}$$

Upon introducing the total disclination density (Kossecka and de Witt 1977)

$$s(\boldsymbol{k}) \equiv -k^2 v(k) = -(k^2\delta_{ij} - k_i k_j)u_{ij}^{\mathrm{T}}(\boldsymbol{k}) = -(k^2\delta_{ij} - k_i k_j)u_{ij}^0(\boldsymbol{k}) \tag{2.11}$$

and transforming back to real space, we find

$$s(\boldsymbol{r}) = \varepsilon_{ik}\varepsilon_{jl}(\partial/\partial x_k)(\partial/\partial x_l)\, u_{ij}^0(\boldsymbol{r}). \tag{2.12}$$

The total disclination density includes both isolated disclinations and dislocations, regarded as disclination dipole pairs. It is simply related to the 'incompatibility' $\eta(\boldsymbol{r})$ used in the continuum elasticity literature (see, e.g. de Witt 1970, 1973)

$$\eta(\boldsymbol{r}) = -s(\boldsymbol{r}). \tag{2.13}$$

Upon inserting (2.7) into (2.12), we find that the total disclination density in the ground state of a surface $f(x, y)$ is

$$s(\boldsymbol{r}) = \varepsilon_{ik}\varepsilon_{jl}(\partial/\partial x_k)(\partial/\partial x_l)[(\partial f/\partial x_i)(\partial f/\partial x_j)\, F(|\nabla f|^2)]. \tag{2.14}$$

In the special case when f is a function only of the radial coordinate $\rho = (x^2 + y^2)^{1/2}$, $f(\rho) = f(x, y)$, the expression (2.14) simplifies to

$$s(\boldsymbol{r}) = 2(\mathrm{d}f/\mathrm{d}\rho)(\mathrm{d}^2 f/\mathrm{d}\rho^2)/\{\rho[1 + (\mathrm{d}f/\mathrm{d}\rho)^2]^{3/2}\}. \tag{2.15}$$

The guassian curvature of this surface is easily found to be

$$K = 2(\mathrm{d}f/\mathrm{d}\rho)(\mathrm{d}^2 f/\mathrm{d}\rho^2)/\{\rho[1 + (\mathrm{d}f/\mathrm{d}\rho)^2]^2\}. \tag{2.16}$$

It follows that

$$K = s\cos\theta \tag{2.17}$$

where θ is the angle between the normal to the surface and the z axis. The total disclination density in the tangent plane to the surface (i.e. $s\cos\theta$) is exactly the gaussian curvature. We shall be interested in random surfaces $f(x, y)$ for which $|\nabla f(x, y)|$ is small. To leading order in ∇f we find from (2.14) that

$$s(\boldsymbol{r}) = -\tfrac{1}{2}\varepsilon_{ik}\varepsilon_{jl}(\partial/\partial x_k)(\partial/\partial x_l)[(\partial f/\partial x_i)\,\partial f/\partial x_j] = \det(\partial^2 f/\partial x_i \partial x_j) = K(\boldsymbol{r}). \tag{2.18}$$

The free energy must be a homogeneous isotropic function of $\tilde{g}_{ij}$. In the harmonic approximation it takes the form (Landau and Lifshitz 1970)

$$F = \frac{1}{2}\int \frac{\mathrm{d}^2 r}{a^2} \frac{\tilde{g}_{ij}}{2} C_{ijkl} \frac{\tilde{g}_{kl}}{2} \tag{2.19}$$

where

$$C_{ijkl} = \mu(\delta_{ik}\delta_{jl} + \delta_{il}\delta_{jk}) + \lambda\delta_{ij}\delta_{kl}. \tag{2.20}$$

Since we have dropped higher-order terms in $\tilde{g}_{ij}$, we must also make the corresponding approximation in (2.2):

$$\tilde{g}_{ij} = \partial u_i/\partial x_j + \partial u_j/\partial x_i + (\partial f/\partial x_i)(\partial f/\partial x_j) = 2u_{ij} + (\partial f/\partial x_i)(\partial f/\partial x_j). \tag{2.21}$$

The free energy we will now work with is

$$F = \frac{1}{2}\int \frac{\mathrm{d}^2 r}{a^2} \left(u_{ij} + \frac{1}{2}\frac{\partial f}{\partial x_i}\frac{\partial f}{\partial x_j}\right) C_{ijkl} \left(u_{kl} + \frac{1}{2}\frac{\partial f}{\partial x_k}\frac{\partial f}{\partial k_l}\right). \tag{2.22}$$

Equation (2.22) agrees with part of an elastic energy discussed by Landau and Lifshitz (1970) describing the equilibrium of a flexible bent plate. Upon freezing such a plate in a particular configuration and allowing the stresses within the plate to relax, one is led to the statistical mechanics problem addressed in this paper. It is important to emphasise that it will not always be possible to compensate the gaussian curvature of a surface by disclination charges in a way suggested by (2.18); disclinations and dislocations in a crystal have quantised charges, and can only approximate a continuous distribution of charge at long wavelengths if they are unbound. The amount of compensation depends on the temperature, and is discussed in detail in § 3.

2.2. *Harmonic theory*

We will now calculate the correlation functions of $\boldsymbol{u}(\boldsymbol{r})$ as given by the free energy (2.22) in the absence of defects. As will be shown in § 3, there is a range of temperatures for weakly fluctuating surfaces where defects can in fact be neglected at long wavelengths. We shall assume that surface fluctuations are described by quenched probability distributions of the form (1.5) or (1.6). Defining the Fourier-transformed variables

$$\tilde{u}_i(\boldsymbol{k}) = \frac{a}{\Omega^{1/2}}\int \frac{\mathrm{d}^2 r}{a^2} u_i(\boldsymbol{r})\, \mathrm{e}^{\mathrm{i}\boldsymbol{k}\cdot\boldsymbol{r}} \tag{2.23a}$$

and

$$\tilde{f}(\boldsymbol{k}) = \frac{a}{\Omega^{1/2}}\int \frac{\mathrm{d}^2 r}{a^2} f(r)\, \mathrm{e}^{\mathrm{i}\boldsymbol{k}\cdot\boldsymbol{r}} \tag{2.23b}$$

the free energy becomes

$$\begin{aligned} F\{\tilde{u};f\} = {} & \tfrac{1}{2}\sum_k \tilde{u}_i(\boldsymbol{k})\, C_{ij}(\boldsymbol{k})\tilde{u}_j(-\boldsymbol{k}) \\ & + \frac{\mu a}{\Omega^{1/2}}\sum_{p,k} (-\mathrm{i})p_i\tilde{f}(\boldsymbol{p})\mathrm{i}(p+k)_j\tilde{f}(-\boldsymbol{p}-\boldsymbol{k})\tfrac{1}{2}(-\mathrm{i})\left(\mathrm{k}_j\tilde{\mathrm{u}}_i(\boldsymbol{k}) + k_i\tilde{u}_j(\boldsymbol{k})\right) \\ & + \frac{\lambda a}{2\Omega^{1/2}}\sum_{p,k} (-\mathrm{i})\,k_i\tilde{u}_i(\boldsymbol{k})(-\mathrm{i})\,p_l\tilde{f}(\boldsymbol{p})\mathrm{i}(p+k)_l\tilde{f}(-\boldsymbol{p}-\boldsymbol{k}) \end{aligned} \tag{2.24}$$

where C_{ij} is the usual elastic quadratic form

$$C_{ij}(\boldsymbol{k}) = \mu k^2(\delta_{ji} - k_i k_j/k^2) + (2\mu + \lambda)(k_i k_j/k^2)k^2. \tag{2.25}$$

We have dropped a term proportional to $|\nabla f|^4$ because it drops out of quenched averages.

To evaluate the correlation functions of $\boldsymbol{u}(\boldsymbol{r}($ it is useful to introduce a source term $J_i(k)$ and evaluate the expression

$$\left[\left\langle \exp\left(\sum_k J_i(-k)\tilde{u}_j(k)\right)\right\rangle\right]_{\mathrm{d}}. \tag{2.26}$$

Here the angular brackets denote a thermal average over the free energy (2.24) and the square brackets denote a quenched average over the disordered surface f. The thermal average in (2.26) is given by

$$\left\langle \exp\left(\sum_k J_i(-k)\tilde{u}_i(k)\right)\right\rangle = \int \mathcal{D}\tilde{u}(k) \exp\left(-F(\tilde{u};\tilde{f}) + \sum_k J_i(k)\tilde{u}_i(k)\right) \Big/ \int \mathcal{D}\tilde{u}(k) \exp(-f\{\tilde{u};\tilde{f}\}) \tag{2.27}$$

where

$$F\{\tilde{u},\tilde{f}\} = \tfrac{1}{2}\sum_k \tilde{u}_i(\boldsymbol{k})C_{ij}(\boldsymbol{k})\tilde{u}_j(-\boldsymbol{k}) + \sum_k \tilde{u}_i(\boldsymbol{k})A_i(-\boldsymbol{k}) \tag{2.28}$$

with

$$A_i(-\boldsymbol{k}) = \frac{\mu a}{2\Omega^{1/2}}\sum_p (-\mathrm{i})k_j\tilde{f}(\boldsymbol{p})\tilde{f}(-\boldsymbol{p}-\boldsymbol{k})(-\mathrm{i})\mathrm{i}[p_i(p+k)_j + p_j(p+k)_i] + \frac{\lambda a}{2\Omega^{1/2}}\sum_p (-\mathrm{i})k_i(-\mathrm{i})p_l\tilde{f}(\boldsymbol{p})\mathrm{i}(p+k)_l\tilde{f}(-\boldsymbol{p}-\boldsymbol{k}). \tag{2.29}$$

The quadratic functional integral in (2.27) is easily carried out, with the result

$$\left\langle \exp\sum_k J_i(-k)\tilde{u}_i(\boldsymbol{k})\right\rangle = \exp\left(\tfrac{1}{2}\sum_k J_i(\boldsymbol{k})C_{ij}^{-1}(\boldsymbol{k})J_j(-\boldsymbol{k}) - \sum_k J_i(\boldsymbol{k})C_{ij}^{-1}(\boldsymbol{k})A_j(-\boldsymbol{k})\right). \tag{2.30}$$

We must now evaluate the average of (2.30) over the probability distributions (1.5) and (1.6). Since $A_j(\boldsymbol{k})$ is quadratic in f, we are led to consider the vertex shown in figure 3(a). The wavy lines represent f-propagators and the straight line is an external source. The average of (2.30) over a gaussian probability distribution is the exponential of the sum of connected graphs:

$$\left[\left\langle \exp\sum_k J_i(-k)\tilde{u}_i(\boldsymbol{k})\right\rangle\right]_{\mathrm{d}} = \exp\left(\tfrac{1}{2}\sum_k J_i(\boldsymbol{k})C_{ij}^{-1}(\boldsymbol{k})J_j(-\boldsymbol{k})\right)\mathrm{e}^S \tag{2.31}$$

where S is given by the graphical series displayed in figure 3(b). The leading 'tadpole' graph is identically zero. All the graphs have equal numbers of vertices and propagators. Each vertex carries one power of momentum for each f-line emanating from it. For the rough surface (1.5), an f-propagator carrying momentum q has a factor $1/q^2$ associated with it. The two powers of q from the two vertices joined by the propagator compensate this $1/q^2$. It follows that all the diagrams for both the rough surface (1.5) and the smooth surface (1.6) are regular for small values of the momenta carried by the external lines.

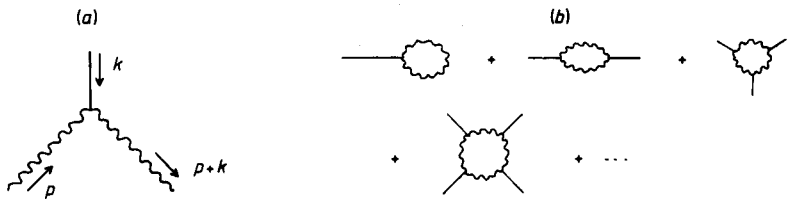

Figure 3. (*a*) A vertex showing the coupling of the f-field (wavy lines) to an external source. (*b*) All the graphs that are generated when the quenched random field f is averaged over.

We will only evaluate the leading terms in an expansion in small values of the external momenta. To this order we can replace the momenta in all the lines in a loop by a single loop momentum p. In this approximation the vertex in figure 3(*a*) reduces to

$$J_i C_{ij}^{-1}(\boldsymbol{k})[(\mu a/\Omega^{1/2})\,(\mathrm{i})k_l p_j p_l + (\lambda a/2\Omega^{1/2})\,(\mathrm{i})k_j p_l p_l]. \tag{2.32}$$

Thus, each vertex carries a power of $1/k$ for small k; a loop with n external lines each carrying a momentum k will behave like $1/k^n$ for small k. From this it is clear that the n-point correlation function of the $\tilde{u}_i(k)$ has exactly the same leading-k behaviour as the harmonic continuum elastic model in flat space. For example, a straightforward calculation of the two-point function, obtained by differentiating (2.31) with respect to the source $J_i(-\boldsymbol{k})$, gives

$$\begin{aligned}\langle \tilde{u}_i(k)\tilde{u}_j(-k)\rangle &= \frac{1}{k^2}\left[\left(\frac{1}{\mu}+\frac{T_f^2}{16\pi}\begin{Bmatrix}\frac{1}{3}\pi^6\\ \pi^2\end{Bmatrix}\right)\left(\delta_{ij}-\frac{k_ik_j}{k^2}\right)\right.\\ &\quad\left.+\left(\frac{1}{2\mu+\lambda}+\frac{T_f^2}{16\pi}\frac{(3\mu^2+4\mu\lambda+2\lambda^2)}{(2\mu+\lambda)^2}\begin{Bmatrix}\frac{1}{3}\pi^6\\ \pi^2\end{Bmatrix}\right)\frac{k_ik_j}{k^2}\right]\\ &\equiv \frac{1}{k^2}\left[\frac{1}{\mu_R}\left(\delta_{ij}-\frac{k_ik_j}{k^2}\right)+\frac{1}{2\mu_R+\lambda_R}\frac{k_ik_j}{k^2}\right]\end{aligned} \tag{2.33}$$

to leading order in k. Here the upper term in the curly brackets refers to the smooth surface (1.6) and the lower term to the rough surface (1.5). Apart from finite renormalisations in the elastic constants, the leading-k behaviour of the two-point function is unchanged.

It is well known that thermal fluctuations have a pronounced effect on correlations in two-dimensional solids (Jancovici 1967). Although conventional long-range order (leading to δ-function Bragg peaks in the structure function) is destroyed, translation correlations exhibit a slow algebraic decay to zero whenever there are non-zero elastic constants. If $\boldsymbol{G}$ is a reciprocal-lattice vector, the relevant correlation function is (see, e.g., Nelson and Halperin 1979)

$$C_G(\boldsymbol{r}) = \langle \exp[\mathrm{i}\boldsymbol{G}\cdot(\boldsymbol{u}(\boldsymbol{r})-\boldsymbol{u}(\boldsymbol{0}))]\rangle \sim 1/r^{\eta_G} \tag{2.34a}$$

with

$$\eta_G = k_B T\,|\boldsymbol{G}|^2\,(3\mu+\lambda)/4\pi\mu(2\mu+\lambda). \tag{2.34b}$$

It is straightforward to show that this result remains valid for crystalline solids on corrugated surfaces, with μ and λ replaced by the renormalised elastic constants appearing in (2.33).

3. Defects

3.1. Free energy

We shall be interested in the energetics of defects in the strain field u_{ij} of the crystal. We take disclinations to be the fundamental defect and we build dislocations out of disclination pairs. The dislocation–disclination theory of melting on a flat substrate can also be formulated in this way (Nelson 1982). If there are disclination charges s_α at positions $\boldsymbol{r}_\alpha$ and dislocation charges $\boldsymbol{b}^\beta$ at positions $\boldsymbol{r}_\beta$, then the total disclination density is

$$s(\boldsymbol{r}) = \sum_\alpha \delta(\boldsymbol{r} - \boldsymbol{r}_\alpha)\, s_\alpha + a_0 \varepsilon_{ij} \sum_\beta b_j^\beta \partial_i\, \delta(\boldsymbol{r} - \boldsymbol{r}_\beta) = \varepsilon_{ik}\varepsilon_{jl} \frac{\partial}{\partial x_k}\frac{\partial}{\partial x_l} u_{ij}. \tag{3.1}$$

Here, a_0 is the lattice constant, and the Burgers vectors $\boldsymbol{b}^\beta$ are dimensionless. The quantity u_{ij} is the singular part of the strain field, induced by the defects. Upon defining

$$e_{ij} = \tfrac{1}{2}\tilde{g}_{ij} = u_{ij} + \tfrac{1}{2}(\partial f/\partial x_i)\,(\partial f/\partial x_j) \tag{3.2a}$$

the free energy (2.22) takes the form

$$F\{e\} = -\tfrac{1}{2}\int \frac{\mathrm{d}^2 r}{a^2}\, e_{ij} C_{ijkl} e_{kl}. \tag{3.2b}$$

It will be convenient to consider a defect density measured relative to the distribution $K(\boldsymbol{r})$ favoured by the gaussian curvature of the surface (see equation (2.18)):

$$d(\boldsymbol{r}) = s(\boldsymbol{r}) - K(\boldsymbol{r}) = \varepsilon_{ik}\varepsilon_{jl}(\partial/\partial x_k)(\partial/\partial x_l)\, e_{ij}. \tag{3.3}$$

Since the displacement fields adjust themselves to find the local minimum of the free energy for any defect density, we have

$$\delta F/\delta u_i = 0 \tag{3.4}$$

which gives, using (3.2b), the condition

$$\partial_i C_{ijkl}\, e_{kl} = 0. \tag{3.5}$$

In order to solve (3.3) and (3.5) for $e_{ij}(\boldsymbol{r})$, we make the substitution

$$e_{kl}(\boldsymbol{r}) = \int \mathrm{d}^2 r'\; G_{kl}(\boldsymbol{r} - \boldsymbol{r}')\, d(\boldsymbol{r}') \tag{3.6}$$

which means that the tensor Green function $G_{kl}(\boldsymbol{r})$ must satisfy

$$\varepsilon_{mk}\varepsilon_{nl}(\partial/\partial x_m)(\partial/\partial x_n) G_{kl}(\boldsymbol{r}) = \delta(\boldsymbol{r}) \tag{3.7a}$$

and

$$\partial/\partial x_i C_{ijkl} G_{kl}(\boldsymbol{r}) = 0. \tag{3.7b}$$

Upon writing

$$G_{kl}(\boldsymbol{r}) = \int \frac{\mathrm{d}^2 k}{(2\pi)^2}\, \tilde{G}_{kl}(\boldsymbol{k})\,(\mathrm{e}^{-\mathrm{i}\boldsymbol{k}\cdot\boldsymbol{r}} - 1) \tag{3.8}$$

we find

$$\varepsilon_{mk}\varepsilon_{nl} k_m k_n \tilde{G}_{kl} = -1 \tag{3.9}$$

and

$$k_i C_{ijkl} \tilde{G}_{kl} = 0. \tag{3.10}$$

Equations (3.9) can be written

$$k^2(\delta_{kl} - k_k k_l/k^2)\, \tilde{G}_{kl} = -1 \tag{3.11}$$

which is solved by

$$\tilde{G}_{kl}(\boldsymbol{k}) = -(1/k^2)[(\delta_{kl} - k_k k_l/k^2) + \alpha k_k k_l/k^2] \tag{3.12}$$

where α is an unknown function of k. Inserting this into (3.10) we obtain

$$\alpha = -\lambda/(\lambda + 2\mu) \tag{3.13}$$

where we have used the isotropic form (2.20) for the elasticity tensor. It follows that

$$G_{kl}(\boldsymbol{r}) = -\int \frac{\mathrm{d}^2 k}{(2\pi)^2} \frac{(\mathrm{e}^{-\mathrm{i}\boldsymbol{k}\cdot\boldsymbol{r}} - 1)}{k^2} \left[\left(\delta_{kl} - \frac{k_k k_l}{k^2}\right) - \frac{\lambda}{\lambda + 2\mu} \frac{k_k k_l}{k^2}\right]$$

$$\underset{r\to\infty}{\simeq} \frac{\mu}{2\pi(\lambda + 2\mu)} \ln \frac{|\boldsymbol{r}|}{a} \delta_{kl} + \frac{(\lambda + \mu)}{2\pi(\lambda + 2\mu)} \frac{r_k r_l}{r^2}. \tag{3.14}$$

We must now insert (3.6) into (3.2*b*) and obtain the free energy for a given defect density. Defining the Fourier transform of $d(\boldsymbol{r})$ as in (2.23) we find

$$F_{\mathrm{d}} = \tfrac{1}{2} \sum_{\boldsymbol{k}} \tilde{d}(-\boldsymbol{k}) d(\boldsymbol{k}) \tilde{G}_{ij}(\boldsymbol{k}) C_{ijkl} \tilde{G}_{kl}(-\boldsymbol{k}). \tag{3.15}$$

One readily finds that

$$\tilde{G}_{ij}(\boldsymbol{k}) C_{ijkl} \tilde{G}_{kl}(\boldsymbol{k}) = (1/k^4)\, 4\mu(\mu + \lambda)/(\lambda + 2\mu) \equiv K_0/k^4. \tag{3.16}$$

Thus the desired defect free energy is

$$F_{\mathrm{d}} = \frac{K_0}{2} \sum_{\boldsymbol{k}} \tilde{d}(-\boldsymbol{k}) \frac{1}{k^4} \tilde{d}(\boldsymbol{k}) + E_{\mathrm{c}} \sum_{\alpha} s_\alpha^2 + E_{\mathrm{p}} \sum_{\beta} |\boldsymbol{b}_\beta|^2. \tag{3.17}$$

Upon allowing for small phonon displacements about a particular disclination configuration, one obtains an additional phonon free-energy contribution already treated in § 2.2. We have inserted phenomenological core energies E_{c} and E_{p} for dislocations and disclinations. These terms arise from non-linear stresses near the core of the defect. Because dislocations are regarded as disclination pairs we expect that $E_{\mathrm{p}} \simeq 2E_{\mathrm{c}}$. We have also used the conditions

$$\int \mathrm{d}^2 r\, d(\boldsymbol{r}) = 0 \tag{3.18*a*}$$

and

$$\int \mathrm{d}^2 r\, \boldsymbol{r}\, d(\boldsymbol{r}) = 0. \tag{3.18*b*}$$

Configurations not satisfying these constraints have energies that diverge with the size of the system. It turns out (see § 3.2) that the curvature contribution to $d(\boldsymbol{r})$ integrates to zero when inserted into (3.18). One is left with disclination and dislocation charge neutrality conditions on thermally activated defects, namely

$$\sum_{\alpha} s^\alpha = 0 \tag{3.19*a*}$$

and

$$a_0 \sum_\beta \boldsymbol{b}^\beta + \sum_\alpha \boldsymbol{r}^\alpha s^\alpha = 0. \tag{3.19b}$$

3.2. Dislocation interactions

We now wish to examine whether it is possible for the dislocations in the crystal to unbind and destroy translational order. We assume we are in a phase where all the disclinations occur only as tightly bound pairs to form dislocations, so all $s_\alpha = 0$ in (3.1), and

$$d(\boldsymbol{r}) = a_0 \sum_\beta \varepsilon_{ij} b_j^\beta \partial_i \delta(\boldsymbol{r} - \boldsymbol{r}_\beta) - K(\boldsymbol{r}). \tag{3.20}$$

Inserting the expression (3.20) into the free energy (3.17) and using the charge neutrality conditions (3.20), we obtain

$$F_d = -\frac{K_0}{8\pi} \sum_{\alpha \neq \beta} \left(\boldsymbol{b}^\alpha \cdot \boldsymbol{b}^\beta \ln \frac{|\boldsymbol{r}_{\alpha\beta}|}{a} - \frac{(\boldsymbol{b}^\alpha \cdot \boldsymbol{R}_{\alpha\beta})(\boldsymbol{b}^\beta \cdot \boldsymbol{R}_{\alpha\beta})}{|\boldsymbol{r}_{\alpha\beta}|^2} \right)$$
$$+ E_p' \sum_\alpha |\boldsymbol{b}^\alpha|^2 - \frac{K_0}{\Omega^{1/2}} \sum_{\beta,k} \frac{\bar{K}(-k)\, \varepsilon_{ij}(-ik)_i b_j^\beta \exp(i\boldsymbol{k} \cdot \boldsymbol{r}_\beta)}{k^4} \tag{3.21}$$

where

$$\boldsymbol{R}_{\alpha\beta} = \boldsymbol{r}_\alpha - \boldsymbol{r}_\beta \qquad E_p' = E_p + CK_0/4. \tag{3.22}$$

The quantity C is the cut-off-dependent constant in the integral

$$\int \frac{d^2k}{(2\pi)^2} \left(\delta_{ij} - \frac{k_i k_j}{k^2} \right) \frac{(e^{i\boldsymbol{k}\cdot\boldsymbol{r}} - 1)}{k^2} \underset{r\to\infty}{\simeq} -\frac{1}{4\pi} \left(\delta_{ij} \ln \frac{r}{a} - \frac{r_i r_j}{r^2} \right) - \delta_{ij} C. \tag{3.23}$$

Note that the surface topography interacts with dislocations in the crystal via the fourier-transformed gaussian curvature. To proceed further we need the quenched probability distribution for the gaussian curvature associated with surfaces described by (1.5) and (1.6).

3.3. The probability distribution for the gaussian curvature

We first consider the generating function

$$X(B) = \left[\exp\left(\sum \tilde{B}(-k) \tilde{K}(k) \right) \right]_d$$
$$= \left[\exp\left\{ -\tfrac{1}{2} \int \frac{d^2r}{a^2} B(r)\, \varepsilon_{mk} \varepsilon_{nl} \frac{\partial}{\partial x_m} \frac{\partial}{\partial x_n} \left(\frac{\partial f}{\partial x_k} \frac{\partial f}{\partial x} \right) \right\} \right]_d \tag{3.24}$$

where $[\ldots]_d$ means an average over the quenched disorder embodied in the surface probability distributions (1.5) or (1.6). Averages of this form repeatedly appear in the statistical mechanics associated with (3.21). Upon integrating by parts in (3.24) we find

$$X(B) = \left[\exp\left(-\tfrac{1}{2} \int \frac{d^2r}{a^2} \varepsilon_{mk} \varepsilon_{nl} \frac{\partial^2 B}{\partial x_m \partial x_n} \frac{\partial f}{\partial x_k} \frac{\partial f}{\partial x_l} \right) \right]_d$$
$$= \left[\exp\left(-\frac{a}{2\Omega^{1/2}} \sum_k \varepsilon_{mk} \varepsilon_{nl} (-ik)_m (-ik)_n (-ip)_k [i(p+k)_l] \right.\right.$$
$$\left.\left. \times B(k) f(p) f(-p-k) \right) \right]_d. \tag{3.25}$$

The structure of this average is exactly the same as that of (2.30)–(2.32). The quantity $X(B)$ is given by the exponential of the connected graphs shown in figure 3(b), with the proviso that the straight external lines now carry factors of $\tilde{B}(k)$. The 'tadpole' graph vanishes as before. Upon making the same small-external-momenta approximations as in § 2.2, we find that the first non-vanishing contribution to the exponential is

$$T_f^2 \frac{B(k)B(-k)a^2}{4\Omega} \varepsilon_{mk}\varepsilon_{nl}k_m k_n \varepsilon_{pr}\varepsilon_{qs} k_p k_q \sum_p p_k p_r p_l p_s \begin{Bmatrix} a^4 \\ 1/p^4 \end{Bmatrix}$$

$$= B(k)B(-k)\frac{3T_f^2}{128\pi}\begin{Bmatrix} \frac{1}{3}\pi^6 \\ \pi^2 \end{Bmatrix} k^4. \tag{3.26}$$

As before the upper term refers to smooth surfaces and the lower term to rough surfaces. It is easy to check that for higher-order graphs, graphs with n external lines behave like $T_f^n k^{2n}$. It follows that for small T_f and external momenta, the two-point graph considered above dominates. In this approximation it is easy to check that correlations in the gaussian curvature are described by the probability distribution

$$\mathcal{P}(\tilde{K}(k)) \propto \exp\left(-\tfrac{1}{2}\frac{64\pi}{3T_f^2}\begin{Bmatrix} 3/\pi^6 \\ 1/\pi^2 \end{Bmatrix} \sum_k \frac{\tilde{K}(k)\tilde{K}(-k)}{k^4}\right). \tag{3.27}$$

3.4. The dislocation-unbinding transition

We are now in a position to determine the renormalisation-group recursion relations associated with the defect free energy (3.22). These are most easily constructed by the replica method used previously for quenched random impurities (Nelson 1983b). Upon introducing replica indices m, n, we use the probability distribution (3.27) to carry out the average over the quenched randomness, with the result

$$F^{\text{replica}} = \frac{-\hat{K}}{8\pi}\sum_{r_\alpha \neq r_\beta}\sum_m \left[\boldsymbol{b}^{\alpha m}\cdot\boldsymbol{b}^{\beta m}\ln\left(\frac{|r_{\alpha m}-r_{\beta m}|}{a}\right) - \frac{\boldsymbol{b}^{\alpha m}\cdot(r_{\alpha m}-r_{\beta\mu})\boldsymbol{b}^{\beta m}\cdot(r_{\alpha m}-r_{\beta m})}{|r_{\alpha m}-r_{\beta m}|^2}\right]$$

$$\times\frac{-\tilde{K}}{8\pi}\sum_{\alpha,\beta}\sum_{m\neq n}\left[\boldsymbol{b}^{\alpha m}\cdot\boldsymbol{b}^{\beta n}\ln\left(\frac{|r_{\alpha m}-r_{\beta n}|}{a}\right) - \frac{\boldsymbol{b}^{\alpha m}\cdot(r_{\alpha m}-r_{\beta n})\boldsymbol{b}^{\beta n}\cdot(r_{\alpha m}-r_{\beta n})}{|r_{\alpha m}-r_{\beta n}|^2}\right]$$

$$+ E_p'\sum_m\sum_\alpha |\boldsymbol{b}^{\alpha m}|^2 \tag{3.28}$$

where

$$\hat{K} = K_0 - \frac{3T_f^2}{64\pi}\begin{Bmatrix} \frac{1}{3}\pi^6 \\ \pi^2 \end{Bmatrix} K_0^2 \tag{3.29a}$$

and

$$\tilde{K} = \frac{-3T_f}{64\pi}\begin{Bmatrix} \frac{1}{3}\pi^6 \\ \pi^2 \end{Bmatrix} K_0^2. \tag{3.29b}$$

As usual in the replica method we want to calculate thermal averages and recursion relations from (3.28) and then take the limit $(m, n)\to 0$. This analysis, however, is

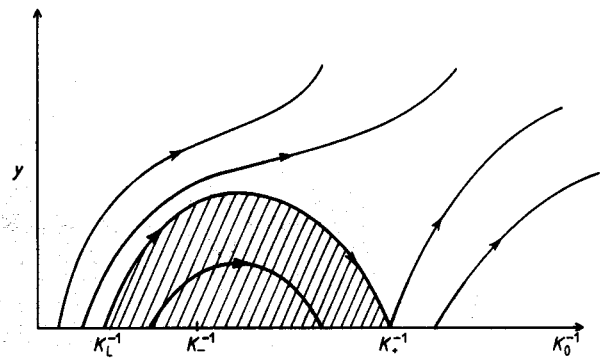

Figure 4. Renormalisation-group flows for the dislocation-unbinding transitions. The shaded portion corresponds to a stable solid phase and flows to large y indicate an instability to the unbinding of dislocations.

formally identical to the defect free energy for quenched random impurities discussed in Nelson (1983b). Upon defining by $\ln y = -E_p'$ the recursion relations may be written

$$dK_0^{-1}/dl = \tfrac{3}{4}\pi \exp[(k_0 - \tilde{\sigma}K_0^2)/8\pi]\{2I_0[(K_0 - \tilde{\sigma}K_0^2)/8\pi] - I_1[(K_0 - \tilde{\sigma}K_0^2)/8\pi]\}y^2 \tag{3.30a}$$

$$dy/dl = [2 - (K_0 - \tilde{\sigma}K_0^2)/8\pi]y + 2\pi \exp[(K_0 - \tilde{\sigma}K_0^2)/16\pi]I_0[(K_0 - \tilde{\sigma}K_0^2)/8\pi]y^2 \tag{3.30b}$$

$$d\tilde{\sigma}/dl = 0 \tag{3.30c}$$

where

$$\tilde{\sigma} = \frac{3T_f^2}{64\pi}\begin{Bmatrix} \frac{1}{3}\pi^6 \\ \pi^2 \end{Bmatrix}. \tag{3.31}$$

For $\tilde{\sigma} < \tilde{\sigma}_c = 1/64\pi$ the Hamiltonian flows are qualitatively like those in figure 4, where

$$K_\pm^{-1} = \frac{1}{32\pi}[1 \pm (1 - 64\pi\tilde{\sigma})^{1/2}]. \tag{3.32}$$

There is a fixed line at $y = 0$. The fixed line is unstable to the formation of dislocations at low temperatures (small K_0^{-1}). This is due to the random topography and represents an attempt to screen out its gaussian curvature. For a range of temperatures between K_L^{-1} and K_+^{-1}, however, $y(l)$ ultimately goes to zero and the crystalline phase is stable. For temperatures below K_L^{-1} the crystal melts re-entrantly into the hexatic phase. For $\tilde{\sigma} > \sigma_c$, i.e. for

$$T_f > \begin{Bmatrix} 1/\pi^3 \\ 1/3^{1/2}\pi \end{Bmatrix} \tag{3.33}$$

the crystalline phase is always unstable toward a dislocation-unbinding transition.

3.5. The disclination-unbinding transition

It was shown by Nelson (1983b) that after the dislocation unbinding, bond orientational order persists and the system has a non-zero stiffness K_A entering an effective free

energy

$$F_A \equiv \tfrac{1}{2} K_A \int d^2r |\nabla\theta|^2. \tag{3.34}$$

Here we examine in a different manner the properties of the system after the dislocations unbind. As in Nelson (1983b) we will treat the dislocations in the 'Debye–Hückel' approximation. In this approximations one integrates, rather than sums, on dislocation degrees of freedom in the partition function for length scales greater than ξ_T. ξ_T is the translational correlational length and diverges as one approaches the solid phase (Nelson and Halperin 1979). We shall assume that the short-wavelength dislocation degrees of freedom have been eliminated by the procedure of § 3.4. Because we are going to integrate degrees of freedom in Fourier space and wish to impose an ultraviolet cut-off of order ξ_T^{-1}, we have to define our Fourier transforms as in (2.23*a*) with a_0 replaced by ξ_T. It is important to note, however, that we retain the factor of a_0 in (3.1), because the size of an elementary dislocation is unchanged. From (3.17) we obtain the effective free energy:

$$F = \frac{1}{2}\frac{K_0 \xi_T^2}{a_0^2} \sum_K \frac{\tilde{d}_{\xi_T}(k)\tilde{d}_{\xi_T}(-k)}{k^4} + E_c \sum_\alpha s_\alpha^2 + E_p \sum_k |\boldsymbol{b}_{\xi_T}(k)|^2 \tag{3.35}$$

with

$$d_{\xi_T}(k) = \frac{1}{\xi_T \Omega^{1/2}} \sum_\alpha s_\alpha e^{i\boldsymbol{k}\cdot\boldsymbol{r}_\alpha} - \tilde{K}_{\xi_T}(k) + \frac{a_0}{\xi_T^2} \varepsilon_{ij}(-ik)_i \tilde{b}_{\xi_T}(k) \tag{3.36}$$

and

$$\boldsymbol{b}_{\xi_T}(k) = \frac{\xi}{\Omega^{1/2}} \sum_\alpha \boldsymbol{b}^\alpha e^{i\boldsymbol{k}\cdot\boldsymbol{r}_\alpha}. \tag{3.37}$$

The subscript ξ_T has been included to emphasise that the Fourier transforms are defined at a length scales longer than ξ_T. Assuming that the timescales of interest are much greater than the time required for the dislocations to equilibrate, we can integrate $\boldsymbol{b}_{\xi_T}(k)$ and find an effective free energy:

$$F_{\text{eff}} = \tfrac{1}{2} \sum_k \left(\frac{1}{\xi_T \Omega^{1/2}} \sum_\alpha s_\alpha e^{i\boldsymbol{k}\cdot\boldsymbol{r}} - \tilde{K}_\xi(k) \right) \left(\frac{k^2 a_0^2}{2E_p \xi_T^4} + \frac{k^4 a_0^2}{K_0 \xi_T^2} \right)^{-1} \times \left(\frac{1}{\xi_T \Omega^{1/2}} \sum_\alpha s_\alpha e^{-i\boldsymbol{k}\cdot\boldsymbol{r}} - \tilde{K}_{\xi_T}(-k) \right) + E_c \sum_\alpha s_\alpha^2. \tag{3.38}$$

For large $\boldsymbol{r}$ (and small $\boldsymbol{k}$) we can ignore the $k^4 a^2 / K_0 \xi_T^2$ term in the denominator and obtain

$$F_{\text{eff}} = -\frac{E_p \xi_T^2}{2\pi a_0^2} \sum_{\alpha \neq \beta} s_\alpha s_\beta \ln \frac{|r_\alpha - r_\beta|}{\xi_T} + E_c' \sum_\alpha s_\alpha^2 - \sum_\alpha \frac{E_p \xi_T^3}{a_0^2 \Omega^{1/2}} \sum_k \tilde{K}_{\xi_T}(-k) \frac{1}{k^2} e^{i\boldsymbol{k}\cdot\boldsymbol{r}_\alpha} \tag{3.39}$$

with

$$E_c' = E_c + \frac{D E_p \xi_T^2}{2a_0^2} \tag{3.40}$$

and where D is the constant in the integral

$$\int^{1/\xi_T} \frac{d^2k}{(2\pi)^2} \frac{e^{i\boldsymbol{k}\cdot\boldsymbol{r}} - 1}{k^2} = -\frac{1}{2\pi} \ln \frac{|r|}{\xi_T} - D. \tag{3.41}$$

We shall assume that factors of $1/kT$ have been absorbed into $F_{\rm eff}$, so the probability of a particular quenched configuration is proportional to $e^{-F_{\rm eff}}$. We will now analyse the free energy (3.39) in the limit of large E_c. First note that the stiffness K_A entering the free energy is proportional to $E_p\xi_T^2/a_0^2$. This agrees with the results of Nelson (1983b). Let $\ln \bar{y} = -E_c'$. It is possible to average over the quenched disorder, embodies in $\tilde{K}_{\xi_T}(k)$, in successive powers of $\bar{y}$. (Equivalent results are obtained using the replica trick; see Rubinstein *et al* 1982.) To lowest order in $\bar{y}$ the quenched average is the same as the annealed average. The probability distribution for $K_{\xi_T}(k)$ from (3.27) is

$$\mathcal{P}(\tilde{K}_{\xi_T}(k)) \propto \exp\left(-\tfrac{1}{2}\frac{64\pi}{3T_f^2}\begin{Bmatrix}3/\pi^6\\1/\pi^2\end{Bmatrix}\sum_k \frac{\tilde{K}_{\xi_T}(k)\tilde{K}_{\xi_T}(-k)}{k^4}\frac{\xi_T^2}{a_0^2}\right). \tag{3.42}$$

It follows that the new effective free energy that results is

$$\tilde{F}_{\rm eff} = -\frac{E_p\xi_T^2}{2\pi a_0^2}\sum_{\alpha\neq\beta} s_\alpha s_\beta \ln\frac{|r_\alpha - r_\beta|}{\xi} + \left(E_c' - \frac{E_p^2\xi_T^2}{a_0^2}\frac{3T_f^2}{128\pi}\begin{Bmatrix}\frac{1}{3}\pi^6\\\pi^2\end{Bmatrix}\right)\sum_\alpha s_\alpha^2. \tag{3.43}$$

The free energy $\tilde{F}_{\rm eff}$ is just the scalar Coulomb gas problem solved by Kosterlitz (1974), with an effective core energy

$$E_c^{\rm eff} = E_c' - \frac{E_p^2 3T_f^2}{128}\begin{Bmatrix}\frac{1}{3}\pi^6\\\pi^2\end{Bmatrix}\frac{\xi_T^2}{a_0^2}. \tag{3.44}$$

Note from (3.40) that E_c' diverges at least as rapidly as ξ_T^2, so positive effective core energies are possible even for large ξ_T. Because E_p and $E_c' \sim 1/T$, however, $E_c^{\rm eff}$ becomes arbitrarily small with decreasing temperatures. As shown by Kosterlitz (1974), there must be a disclination-unbinding transition in this limit. This instability can pre-empt the low-temperature hexatic phase completely for sufficiently large T_f. The two possible equilibrium phase diagrams suggested by this analysis are shown in figure 2.

This mechanism for destabilising the hexatic phase at low temperatures should also apply to solids with quenched random impurities, a possibility that was overlooked by Nelson (1983b). In practice, however, it may be very difficult for disclinations to remain in equilibrium during cooling, in contrast to dislocations, which can equilibrate rapidly via glide diffusion. Unless the cooling rate is very slow, systems with phase diagrams like that in figure 2(*a*) may become trapped in non-equilibrium hexatic configurations at low temperatures.

Acknowledgments

One of us (SS) would like to thank E Brézin for useful comments and encouragement. We have also benefited from conversations with B I Halperin and J F Sadoc. This work was supported by the National Science Foundation through the Harvard Materials Science Laboratory, and through Grant No DMR-82-07431.

References

Arnowitt A B, Deser C D and Misner E F 1962 *Gravitation: an Introduction to Current Research* ed. L Witten (New York: Wiley)

Coexeter H S M 1969 *Introduction to Geometry* (New York: Wiley)

—— 1973 *Regular Polytopes* (New York: Dover)

Gaspard J P, Mosseri R and Sadoc J F 1982 *Proc. Conf. Structure of Non-Crystalline Materials (Cambridge, UK) 1982*
Halperin B I and Nelson D R 1978 *Phys. Rev. Lett.* **41** 121 (Erratum **41** 519)
Jancovici B 1967 *Phys. Rev. Lett.* **19** 20
Kleman M and Sadoc J F 1979 *J. Physique Lett.* **40** L569
Kosevich A M 1979 *Dislocations in Solids* vol 1, ed. F R N Nabarro (Amsterdam: North-Holland) pp 33–141
Kossecka E and de Witt R 1977 *Arch. Mech.* **29** 633
Kosterlitz J M 1974 *J. Phys. C: Solid State Phys.* **7** 1064
Kroner 1981 *Physics of Defects* ed. R Balian, M Kléman and J Poirier (Amsterdam: North-Holland)
Landau L D and Lifshitz E M 1970 *Theory of Elasticity* (New York: Pergamon) pp 58–61
Mattis D C 1976 *Phys. Lett.* A **56** 421
Nelson D R 1982 *Phys. Rev.* B **26** 269
—— 1983a *Phys. Rev.* B **28** 5515
—— 1983b *Phys. Rev.* B **27** 2902
Nelson D R and Halperin B I 1979 *Phys. Rev.* B **19** 2457
Nelson D R, Rubinstein M and Spaepen F 1982 *Phil. Mag.* A **46** 105
Nelson D R and Widom M 1984 *Nucl. Phys.* B **240** [FS 12] 113
Rubinstein M and Nelson D R 1983 *Phys. Rev.* B **28** 6377
Rubinstein M, Shraiman B and Nelson D R 1982 *Phys. Rev.* B **27** 1800
Sethna J 1983 *Phys. Rev. Lett.* **51** 2198
Steinhardt P J, Nelson D R and Ronchetti M 1983 *Phys. Rev.* B **28** 784
de Witt R 1970 *Fundamental Aspects of Dislocation Theory* NBS Special Publication 317, vol 1, ed. J A Simmons, R de Witt and R Bullough (Washington, DC: US Government Printing Office)
—— 1973 *J. Res. NBS* A **77** 49
Yonezawa F and Ninomiya T (eds) 1983 *Topological Disorder in Condensed Matter* (Berlin: Springer)
Young A P 1979 *Phys. Rev.* B **19** 1855
Weeks J A 1980 *Ordering in Strongly Fluctuating Condensed Matter Systems* ed. T Riste (New York: Plenum) p 293